Towards a smoothed particle hydrodynamics algorithm for shocks through layered materials

EINDHOVEN UNIVERSITY OF TECHNOLOGY
Department of Mathematics and Computer Science

CASA-Report 13-09
May 2013

Towards a smoothed particle hydrodynamics algorithm for shocks through layered materials

by

I. Zisis, B.J. van der Linden, C.G. Giannopapa

Centre for Analysis, Scientific computing and Applications
Department of Mathematics and Computer Science
Eindhoven University of Technology
P.O. Box 513
5600 MB Eindhoven, The Netherlands
ISSN: 0926-4507

Proceedings of the 2013 ASME Pressure Vessels & Piping Conference
PVP-2013
July 14-18, 2013, Paris, France

PVP2013-97345

TOWARDS A SMOOTHED PARTICLE HYDRODYNAMICS ALGORITHM FOR SHOCKS THROUGH LAYERED MATERIALS

Iason Zisis[1,2], **Bas van der Linden**[2,3], **Christina Giannopapa**[2]
[1]Materials innovation institute, The Netherlands
[2]Dept. of Mathematics and Computer Science, Eindhoven University of Technology, The Netherlands
[3]Laboratory for Industrial Mathematics Eindhoven, LIME, The Netherlands

ABSTRACT

Hypervelocity impacts (HVIs) are collisions at velocities greater than the target object's speed of sound. Such impacts produce pressure waves that generate sharp and sudden changes in the density of the materials. These are propagated as shock waves. Previous computational research has given insight into this shock loading for the case of homogeneous materials. Shock-wave propagation through materials with discontinuous density distribution has not been considered in depth yet.

Smoothed Particle Hydrodynamics (SPH) is a numerical technique, which has been extensively used for the simulation of HVIs. It is especially suitable for this purpose as it describes both the solid and fluid-like behavior effectively as well as the violent breakup of the material under impact. In previous studies on SPH, impact loading of composite materials was modeled by homogenization of the material, or under assumption of being a so-called functionally graded material (FGM). Both these models neglect the reflection-transmission effects on the interface between materials of different density.

In this paper the shock loading of layered materials is studied. A modification to the standard SPH method is developed and tested, that incorporates materials with purely discontinuous density distribution. The developed method's performance at simple shock loading cases is investigated; reflection-transmission patterns of shock-waves through layered materials are discussed, along with a parametric study of the governing parameters.

NOMENCLATURE

Symbol	Definition
α_u, α_ρ	Dissipative terms coefficients
η	Smoothing length factor
Π_{ij}, Φ_{ij}	Artificial terms
ρ, ρ_o, $\bar{\rho}$	Density, reference density, mean density
σ, τ, p	Total, deviatoric, normal stress element
c, $\bar{c}$	Speed of sound, mean speed of sound
Ca	Cauchy number
h, $\bar{h}$	Smoothing length, mean smoothing length
i, j	Particle indices
K	Bulk modulus
m	Particle mass
N	Total number of particles
t, δt	Time, time step
u, u_{impact}	Velocity, impact velocity
V	Particle volume
W	SPH interpolation kernel
x, δx	Position, spacing

INTRODUCTION

Spacecraft in orbit run the risk to experience impacts from small-sized particles such as space debris and micrometeoroids. Travelling at typical velocities of 10 km/s, micron-sized particles produce degradation of the spacecraft's shield protection. Millimeter or centimeter sized bodies can puncture vital components of the spacecraft or lead to its complete destruction [1].

Materials and configurations for spacecraft shields were considered thoroughly [2] even before the first satellite was set in orbit around the Earth. Multi-component materials are being used [3] extensively.

These Hypervelocity Impact (HVI) events are characterized by the projectile's velocity being higher than the target's material speed of sound. Sharp density changes occur, propagated through the target as shock waves. The projectile's momentum is absorbed, visible by the fact that dynamic pressure is abruptly transformed into static pressure. Normal stress effects on an incremental element of the material overweight the deviatory stress effects and hydrodynamic loading regime occurs [4, 5]. Solid materials will effectively behave like fluids in this loading regime. For these reasons, HVIs are considered to be substantially different than ballistic impacts, where impact velocities are an order of magnitude lower.

In the case of multi-component materials, shock waves will not propagate undisturbed through the specimen. The transition from one layer to its adjacent layer is not a smooth function of space; it shows up as a discontinuity in the density distribution of the target and reflections-transmissions will occur, whenever a shock encounters a material interface [6]. Hence, the shock loading problem becomes a multiphase shock problem.

Due to the fact that experimental data of HVIs are difficult to be obtained in situ, computational methods have been widely used, providing insight into the short time scale processes taking place during impact and data to build efficient shielding structures.

In the first attempts to simulate HVIs, so-called *hydrocodes* were used. These are solution strategies based on solving the conservation equations with the stress tensor decomposed into a hydrodynamic and a deviatoric part. A shock capturing method, such as artificial viscosity or a Riemann solver, is employed to solve for the strong wave propagation problem [5].

Peak pressures of 300 GPa, compressive strains of 50% in the aluminum, and temperatures in the order of 10,000 K are predicted numerically, by the impact of a 10 km/s tungsten projectile into an aluminum target. The timescale of the rise of these shocks is in the order of magnitude of microseconds [4]. With pressures reaching thousand times the yield strength of materials under study, it was quite relevant for the initial HVI codes to discard the effects of the deviatoric stresses in favor of only the hydrostatic [4,5], at least for the first stages of the process. Thus, shock dynamics is a core subject in the study of HVIs.

With the Smoothed Particle Hydrodynamics (SPH) numerical method, the disintegration of materials under impact is described without severe algorithmic complexity, compared to other methods like Finite Elements Method (FEM) [5]. Its applicability has been advocated in the original simulation of HVI events into monolithic materials by Libersky et al. [7]. Later combined numerical and experimental works established the method as the state-of-the-art tool for HVI simulations [8,9]. The necessity of a special interface algorithm to treat non-bonded interfaces (e.g. projectile/target) was underlined by Johnson et al. [10], claiming that when two bodies exchange momentum through simple SPH kernel interaction large errors are produced; this observation was studied by Campbell et al. [11]. Furthermore, SPH has also been combined with the FEM [10], in cases where the impact velocities were closer to the ballistic limit rather than in the HVI regime.

In all previously mentioned studies, the type of artificial viscosity introduced by Monaghan and Ginold [12] is used as a means to remove the spurious oscillations in the vicinity of the shocks. An alternative shock capturing technique is the implementation of a Riemann solver in the SPH scheme; such SPH algorithms are described by Intuska [13] and Cha et al. [14]. In a similar manner, an SPH scheme based on the acoustic approximation of the Riemann problem is developed by Parshikov et al. [15].

Multi-material shields for spacecraft are preferred to monolithic ones, because of their lower weight-to-performance ratio [3,16-18] and efforts were made to simulate HVIs into multi-component structures with SPH. Homogenized materials were introduced, with properties the averaged properties of their components. The homogenization approach became popular in the HVI community and was equipped with a rigorous procedure of producing averaged versions of anisotropic materials [16-18]. Nevertheless, two major drawbacks are apparent in this approach: the homogenization process is based on assumptions coming from quasi-static loading regimes, and the effects of shock reflection-transmission are neglected.

Although, SPH algorithms for multi-material simulations have been published [19–21], they concentrate on incompressible flow regimes. In another approach, the Modified-SPH method is introduced [22] to solve an elastic wave propagation problem through a functionally graded material. The properties of such a material are smooth functions of space. Therefore, without any discontinuities in the properties of the material it is impossible for any transmission-reflection pattern to occur.

An improvement to the standard SPH algorithm is developed in the present paper, such that one-dimensional shock loading of materials with purely discontinuous density profile can be modeled. In addition to that, the new algorithms' functionality for paradigms involving real materials is presented.

MATHEMATICAL MODEL

Commonly, hypervelocity impacts are described through continuum mechanics. In particular, the conservation equations for mass, momentum and energy are used as in hydrodynamics [4,5].

The governing equations written in a Lagrangian frame of reference are:

$$\frac{D\rho}{Dt} = -\rho\frac{\partial u^{\alpha}}{\partial x^{\alpha}}\,, \frac{Du}{Dt} = \frac{1}{\rho}\frac{\partial \sigma^{\alpha\beta}}{\partial x^{\alpha}}\,, \frac{De}{Dt} = -\frac{\sigma^{\alpha\beta}}{\rho}\frac{\partial u^{\alpha}}{\partial x^{\beta}}\,,$$

$$\frac{dx^{\alpha}}{dt} = u^{\alpha} \quad \text{for } \alpha,\beta = 1,2,3, \tag{1}$$

where superscripts indicate the directional index and stresses σ are composed by a normal and a deviatoric part as $\sigma^{\alpha\beta} = -p\delta_{\alpha\beta} + \tau^{\alpha\beta}$, where $\delta_{\alpha\beta}$ is the Kronecker delta.

In order to provide a simple case for benchmarking the currently proposed SPH method and since the shock effects are under study, the Euler equations in one dimension are adopted. They describe the flow of compressible media, allowing for shock formation. Since in one dimension only "normal" stresses p are exerted, no distinction can be made between fluids and solids.

Under the assumption of isothermal processes, the thermal energy equation from (1) is neglected.

$$\frac{D\rho}{Dt} = -\rho\frac{\partial u}{\partial x}\,, \qquad \frac{Du}{Dt} = -\frac{1}{\rho}\frac{\partial p}{\partial x}\,, \qquad \frac{dx}{dt} = u\,. \tag{2}$$

A linear Equation of State (EoS), describes a compressible elastic structure consisting of spatially varying material properties that is a bulk modulus constant in time. Pressure from a reference density $\rho_o = \rho(x,0)$ is given as in [5]:

$$p(x,t) = K(x)\left(\frac{\rho(x,t)}{\rho(x,0)} - 1\right). \tag{3}$$

The following dimensionless magnitudes transform (2) into its non-dimensional form:

$$x^* := x/L\,, t^* := t/\tau\,,\ u^* := u/u_o,$$

$$\rho^* := \rho/\rho_o\,, p^* := p/p_o\,. \tag{4}$$

Choosing timescale $\tau = L/u_o$ and pressure scale $p_o = \rho_o u_o^2 = \rho(x,0)u_o^2$ the non-dimensional form of (2) is identical to itself. Dividing (3) by p_o, the non-dimensional EoS becomes:

$$p^* = \frac{K(x)}{\rho(x,0)u_o^2}(\rho^* - 1) = \frac{1}{\mathrm{Ca}(x)}(\rho^* - 1)\,, \tag{5}$$

where

$$\mathrm{Ca}(x) := \frac{\rho(x,0)u_o^2}{K(x)} \tag{6}$$

is the Cauchy number. It is a spatially varying dimensionless quantity, measuring the ratio of the initial inertial forces over the resistance of the materials to compression.

After removing all asterisks, the system of equations looks similar to (2):

$$\frac{D\rho}{Dt} = -\rho\frac{\partial u}{\partial x}\,, \qquad \frac{Du}{Dt} = -\frac{1}{\rho}\frac{\partial p}{\partial x}\,, \qquad \frac{dx}{dt} = u\,, \tag{7a}$$

$$p(x,t) = \frac{1}{\mathrm{Ca}(x)}(\,\rho(x,t) - 1\,)\,. \tag{7b}$$

Given the compressibility effects produced by the projectile's inertia on the target, the bulk modulus $K(x)$ scales with the dynamic pressure at the moment of impact. Therefore, a suitable choice for the velocity scale is $u_o = u_{\mathrm{impact}}$; the relative velocity at which projectile and target travel.

Typical length scales of targets in HVIs are in the order of millimeters to centimeters [3]. Velocity scales with the relative impact velocity u_{impact}. Considering a HVI of u_{impact} = 10 km/s and L = 1 cm, the time-scale is brought down to τ = 1 μsec. For Aluminum 2045-T4 the magnitude of Ca for a 10 km/s impact is computed; with a nominal density ρ_o = 2,700 kg/m^3 and K = 73 GPa, Ca = 3.7 is found, according to (6).

The material's non-dimensional speed of sound c is defined in [5] as:

$$c(x) = \sqrt{dp/d\rho} = \mathrm{Ca}(x)^{-1/2}\,. \tag{8}$$

DISCRETIZATION

The continuous system of equations (7) is solved with the SPH method, along with the relevant initial and boundary conditions. Firstly, the standard algorithm is presented. Secondly, a new approach to treat interfaces within the SPH context is introduced.

Standard SPH

In the SPH method, media are discretized into particles that carry the properties of the material and move at the same velocity as the material velocity. Each particle has a certain volume $V_i := \delta\mathbf{x}_i$ coming from the approximation of the integral:

$$\langle f(\mathbf{x})\rangle \approx \sum_{j=1}^{N} f_j\, \mathrm{W}(\mathbf{x}_i - \mathbf{x}_j, h)\, \delta\mathbf{x}_i\,. \tag{9}$$

The concept of a constant-in-time particle mass $m_i := \rho_i V_i$ is introduced [7], based on the varying-in-time particle's density ρ_i and volume V_i. The interpolation formula for the function's spatial derivative is:

$$\left\langle \frac{\partial f(\mathbf{x}_i)}{\partial \mathbf{x}_i} \right\rangle \approx \sum_{j=1}^{N} f_j \frac{\partial \mathrm{W}(\mathbf{x}_i - \mathbf{x}_j, h)}{\partial \mathbf{x}_i} \frac{m_j}{\rho_j} \,. \tag{10}$$

The Gaussian function is chosen as the interpolation kernel, with a scaling such that $\sum_1^N W(\mathbf{x}_i - \mathbf{x}_j, h)\, V_j = 1$ inside the computational domain:

$$W_{ij} = \frac{1}{h\sqrt{\pi}} exp\left\{ -\left(\frac{x_i - x_j}{h} \right)^2 \right\} , \tag{11}$$

where h is the smoothing length.

The following equations are obtained with the SPH discretization of the system (6). A detailed derivation is found in [7,8,12].

$$\left(\frac{D\rho}{Dt} \right)_i = \rho_i \sum_{j=1}^{N} \frac{m_j}{\rho_j} (u_i - u_j) \frac{\partial W_{ij}}{\partial x_i} \tag{12}$$

$$\left(\frac{Du}{Dt} \right)_i = -\frac{1}{\rho_i} \sum_{j=1}^{N} \frac{m_j}{\rho_j} (p_i + p_j + \Pi_{ij}) \frac{\partial W_{ij}}{\partial x_i} \tag{13}$$

$$p_i = \frac{1}{\mathrm{Ca}_i} (\rho_i - 1) \tag{14}$$

$$\frac{dx_i}{dt} = u_i \tag{15}$$

For the momentum equation, expression (13) involving the sum of pressures is suggested in [17] for multi-phase computations.

The artificial viscosity term Π_{ij} dampens unphysical oscillations near shocks. It was introduced by Monaghan [12] and used for HVI simulations by Libersky et al. [7]. It is defined by:

$$\Pi_{ij} = \begin{cases} \dfrac{-\alpha_u \bar{c}_{ij} \mu_{ij} + \beta_u \mu_{ij}^2}{\bar{\rho}_{ij}} \,, (u_i - u_j)(x_i - x_j) < 0 \\ 0 \quad , \quad \text{elsewhere} \end{cases} \tag{16a}$$

$$\mu_{ij} = \frac{h(u_i - u_j)(x_i - x_j)}{(x_i - x_j)^2 + 0.01h^2} \,, \tag{16b}$$

where $\bar{\rho}_{ij} = (\rho_i + \rho_j)/2$, $\bar{c}_{ij} = (c_i + c_j)/2$, $\alpha_u = 1$, $\beta_u = 2$.

For the cases tackled in this paper, free boundary conditions are considered, discontinuous initial data and a discontinuous parameter Ca.

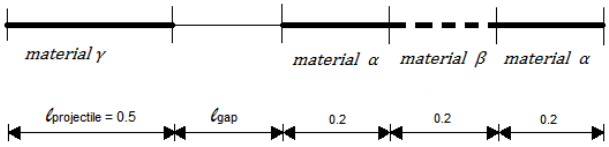

Figure 1 – Initial configuration of the materials

Material	Initial position x_o	Velocity u
α	$0.5 + \ell_{\mathrm{gap}} \le x_o < 0.7 + \ell_{\mathrm{gap}}$	-0.5
β	$0.9 + \ell_{\mathrm{gap}} \le x_o < 1.1 + \ell_{\mathrm{gap}}$	-0.5
γ	$0 \le x_o < 0.5$	0.5

Table 1 – Material's initial positions and velocities

The initial configuration of the materials is depicted on Fig.1. With ℓ_{gap} the initial gap between materials γ (projectile) and α is denoted. The length of the projectile $\ell_{\mathrm{projectile}}$ is chosen large enough so that no effects from rebounded waves occur.

The SPH particle system is initialized by distributing N particles over the domain that the materials initially occupy (Table 1). The initial interparticle distances are taken to be of equal length δx_o. Particles of materials with different density, α and β, have proportional masses as $m_\alpha/m_\beta = \rho_\alpha/\rho_\beta$; these, remain constant in time.

After a number of particles per unit length n_ℓ is defined, the particles are distributed over initial positions $x_{o,i}$, according to the following scheme:

$$\delta x_o = (\ell - \ell_{\mathrm{gap}})/n_\ell \,, \qquad x_{o,i} = \delta x_o (i-1) \tag{17a}$$

$$x_{o,i} = \begin{cases} (i-1)\delta x_o & \text{if } i < \ell_{\mathrm{projectile}}/N \\ (i-1)\delta x_o + \ell_{\mathrm{gap}} & \text{elsewhere} \end{cases} , \tag{17b}$$

where ℓ is the total length of the computational domain considered.

Updates of variables and particle positions in time are achieved via the following scheme. Magnitudes are obtained in the order presented. Braces denote simultaneous update of the enclosed variables and superscripts are reserved for time steps, while subscripts for particle indices. Advancing half a time-step for density and velocity from the initial conditions:

$$\{\rho, u\}_i^{1/2} = \{\rho, u\}_i^0 + \frac{1}{2} \delta t \left(\frac{D\{\rho, u\}}{Dt} \right)_i^0 \tag{18a}$$

and a full-step for position:

$$x_i^1 = x_i^0 + \delta t \, u_i^{1/2} \,. \tag{18b}$$

At every subsequent time step k variables are updated according to:

$$\{\rho,u\}_i^k = \{\rho,u\}_i^{k-1/2} + \frac{1}{2}\delta t\left(\frac{D\{\rho,u\}}{Dt}\right)_i^{k-1}, \quad (18c)$$

where $\left(\frac{D\{\rho,u\}}{Dt}\right)_i^k$ is calculated for each i-th particle according to (12) − (14) and (16).

$$\{\rho,u\}_i^{k+1/2} = \{\rho,u\}_i^{k-1/2} + \delta t\left(\frac{D\{\rho,u\}}{Dt}\right)_i^k, \quad (18d)$$

$$x_i^{k+1} = x_i^k + \delta t\, u_i^{k+1/2}. \quad (18e)$$

A limit to the time-step size is set by the CFL criterion, which by taking the smoothing length as the shortest spatial scale (similarly to [7,8,12]) gives:

$$\delta t \le \omega \min\left(\frac{h}{c_i + u^*_{\text{impact}}}\right), \quad (19)$$

where $\omega \in (0, 1]$ is a "safety" parameter. Computing c_i from (8) and for the non-dimensional u^*_{impact}= 1 (u_{impact} is the velocity scale) it was found sufficient to keep δt = 10^{-4} constant at for all cases solved. For the worst case scenario studied later (highest initial density and Ca product), it reaches δt~0.001 .

The smoothing length is initially taken as $h = \eta V_o = \eta \delta x_o$, with η = 1.2 or 1.3, as suggested by Price [23] for gas shock tube scenarios and Colagrossi et al. [21] for the incompressible multiphase regime, respectively. Although no significant discrepancies in the results were observed when using the two values, $\eta = 1.2$ was preferred, similarly to [23], where compressible phenomena are studied, as well. For the variable smoothing length formulation, it was computed for every particle [9] and updated with an Euler forward scheme, as:

$$\left(\frac{dh}{dt}\right)_i = -\frac{h_i}{\rho_i}\left(\frac{D\rho}{Dt}\right)_i, \quad (20a)$$

$$h_i^{n+1} = h_i^n + \delta t\left(\frac{dh}{dt}\right)_i^n. \quad (20b)$$

Following [7], in the varying smoothing length formulation, the average smoothing length of two particles $\bar{h}_{ij} = (h_i + h_j)/2$ replaces h in (16a).

New SPH term for interface treatment

To capture shocks in gas dynamic simulations with SPH, Price [23] and Monaghan [24] suggest a generalized way to introduce dissipative terms for the balance equations (1). By Θ each variable on the left hand side of (1) is represented:

$$\left(\frac{D\Theta}{Dt}\right)_{i,diss} = \sum_{j=1}^{N} m_j \frac{\alpha_\Theta\, v_{sig}^\Theta}{\bar{\rho}_{ij}}(\Theta_i - \Theta_j)\, r_{ij}\, \frac{\partial W_{ij}}{\partial x_i},$$

$$r_{ij} = \frac{x_i - x_j}{|x_i - x_j|}, \quad (21)$$

where a_Θ is a parameter and v_{sig}^Θ is the propagation speed of the information carried by the dissipative terms. These terms have been used only for the solution of the momentum and energy equations.

The following discussion, presents a new term, developed in order to smoothen out spurious blips in density and pressure, for a shock through a material interface.

Using equation (21), an artificial term is added in the discretized continuity equation (12):

$$\left(\frac{D\rho}{Dt}\right)_i = \rho_i \sum_{j=1}^{N} \frac{m_j}{\rho_j}(u_i - u_j)\frac{\partial W_{ij}}{\partial x_i} + \left(\frac{D\rho}{Dt}\right)_{i,diss},$$

$$\left(\frac{D\rho}{Dt}\right)_{i,diss} = \sum_{j=1}^{N} \frac{\alpha_\rho\,(p_i - p_j)}{\bar{c}_{ij}} \frac{m_j}{\rho_j} r_{ij} \frac{\partial W_{ij}}{\partial x_i}. \quad (22)$$

Unphysical oscillations occur in pressure, while density discontinuities are natural characteristics of inhomogeneous materials. Therefore, an expression in the same manner as (21) needs to account for pressure differences. Exploiting (14), (21) is written as:

$$m_j \frac{\alpha_\rho\, v_{sig}^\rho}{\bar{\rho}_{ij}}(\rho_i - \rho_j) = m_j \frac{\alpha_\rho\, v_{sig}^\rho}{\bar{\rho}_{ij}}\left(\frac{p_i}{c_i^2} - \frac{p_j}{c_j^2}\right), \quad (23)$$

for $v_{sig}^\rho = \bar{c}_{ij}$. Averaging of the density of different materials is not favorable, because this means smoothening of the natural material interfaces, $m_j/\bar{\rho}_{ij}$ is replaced with m_j/ρ_j . With a further approximation the final form is furnished:

$$m_j \frac{\alpha_\rho\, v_{sig}^\rho}{\bar{\rho}_{ij}}\left(\frac{p_i}{c_i^2} - \frac{p_j}{c_j^2}\right) \approx \frac{\alpha_\rho\,(p_i - p_j)}{\bar{c}_{ij}} \frac{m_j}{\rho_j} = \Phi_{ij}, \quad (24)$$

The Φ_{ij} dissipation term (23) is designed such that it smoothens out the spurious blips of density and pressure, occurring on the interface of two materials, similarly to the effect of Π_{ij} on the oscillations of the velocity.

RESULTS AND DISCUSSION

Firstly, a comparison between the standard SPH and the newly proposed algorithm is made with a test case. Due to the impact-induced shock and the large strains around the impact point, the initial regular particles' spacing is

corrupt. The variation of h according to (20) was found to be beneficial to the preservation of the particles' regular spacing and consequently the proper approximation. Therefore, it was used in all cases.

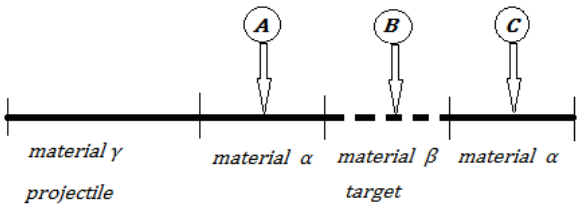

Figure 2 – Initial configuration of the materials in the Cases studied and positions of the gauges.

Secondly, the performance of the algorithm is presented for cases involving real materials. The initial gap is taken ℓ_{gap}= 0, for direct comparison over time elapsed among all cases. Additionally, the projectile's material (material γ) is chosen to be the same as the target's first material (material α) in order to focus on the shock reflection-transmission taking place between layers of the layered structure and not the impact point. The local material velocity of each material is recorded at three points (A,B and C), which are initially in the middle of each layer (Fig.2) and they move along with the material.

All cases were run for n_ℓ = 400 particles per unit length, corresponding to δx_o= 0.0025. This is consistent to the amount of particles per unit length taken from Monaghan [12] in the original shock tube problem with SPH.

Test case

Material	Density	Ca
α	1.0	1.0
β	0.5	0.25
γ	1.0	1.0

Table 2 – Data for the test case

The data from Table 2 are applied for initial gap ℓ_{gap}= 0. Two shock waves are observed traveling away from the impact point. The left shock wave is running undisturbed through the projectile, while the right encounters the interface of the two materials. When it reaches the interface, a reflected and a transmitted wave appears. The transmitted wave continues towards the successive high density layer, from where two other waves are generated, a reflected and a transmitted.

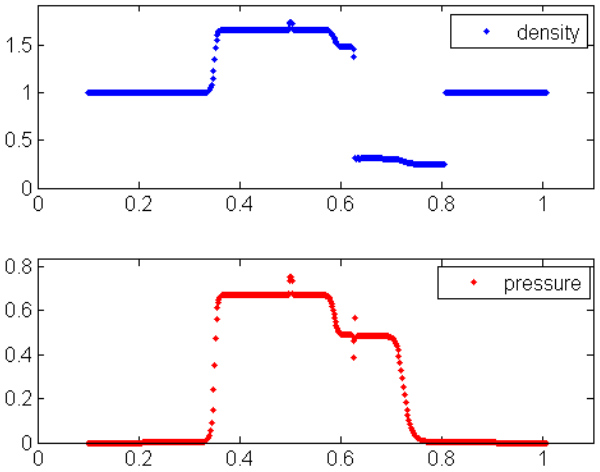

Figure 3 – Test Case without dissipation in the continuity equation, at t = 0.2.

With the standard algorithm, an overshoot in both the density and the pressure, is observed at the impact point (Fig.3). Additionally, a blip in the pressure on the interface occurs. A significant amount of effort in the older [24] and the concurrent [23] SPH literature is devoted at removing such unphysical irregularities, on the interface of two materials under shock.

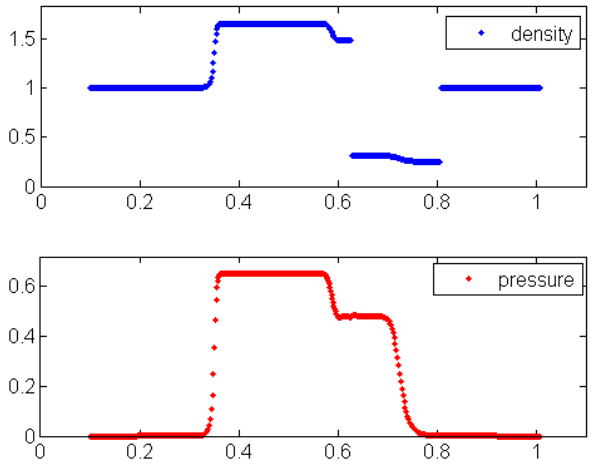

Figure 4 – Test Case with dissipation in the continuity equation, at t = 0.2.

When the dissipation term (25) is applied to the continuity equation, with α_ρ= 0.3, the previous effects disappear (Fig.4).

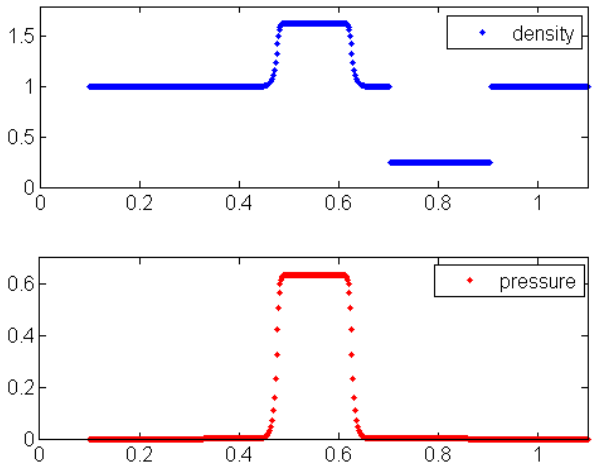

Figure 5 – Test Case, with initial gap $\varepsilon = 0.1$, at $t = 0.2$.

In contrast to Campbell et al. [11], where penetration of particles from one colliding material into the other, justified the use of a contact algorithm, no penetration from the right material into the left material was observed with the new algorithm.

With regard to the optimal value of the artificial term's constant, this was found to be $\alpha_\rho = 0.3$, when no initial gap between projectile and target is present ($\ell_{\text{gap}} = 0$). Results are depicted on Fig.4. It was observed however, that its optimal value depends on the initial gap ℓ_{gap}. Therefore, $\alpha_\rho = 0.8$ was needed for the test case run for Table 2 data and initial gap $\ell_{\text{gap}} = 0.1$ (Fig.5). From all the test cases run, it was evident that the optimal value is $\alpha_\rho \in [0.3, 0.8]$ corresponding to $\ell_{\text{gap}} \in [0, \infty)$. This value was not found to be sensitive to changes in the smoothing length factor in the range $\eta \in [1.2, 1.3]$.

Alternatives for the SPH interpolation kernel were tested; quartic, cubic and quadratic splines, along with a truncated Gaussian from Liu et al. [25] were employed. The kernel was found to affect only the magnitude of the post-shock density at the impact point and not the behavior of the suggested artificial term. In order to choose the optimal kernel, a comparison with a benchmark case is needed. Since the problem is studied in a semi-infinite domain (simulations were stopped when shocks reached the boundaries) the Gaussian was preferred, as in the original shock tube paper [12].

Density ratios resolved by the new algorithm are expected to have a lower limit. In Colagrossi et al. [21], where the weakly compressible regime is studied, the limit for the standard SPH algorithm is stated to be 0.01. This limit was not studied, since for common engineering materials is usually larger than 0.1.

Four different configurations for the layered material are examined (Table 3) for the time frame $t \in [0, 0.75]$. Ca numbers are calculated based on $u_{\text{impact}} = 10$ km/s.

Al-glass-Al

	Material	Density (kg/m^3)	Ca
α	Aluminum 2045-T4	2,700	3.7
β	Glass-filled Epoxy (35%)	1,900	7.6
γ	Aluminum 2045-T4	2,700	3.7

Al-carbon-Al

	Material	Density (kg/m^3)	Ca
α	Aluminum 2045-T4	2,700	3.7
β	Carbon Epoxy (61%)	1,900	1.1
γ	Aluminum 2045-T4	2,700	3.7

St-glass-St

	Material	Density (kg/m^3)	Ca
α	Steel, AISI 1045	8,000	3.9
β	Glass-filled Epoxy (35%)	1,900	7.6
γ	Steel, AISI 1045	8,000	3.9

St-carbon-St

	Material	Density (kg/m^3)	Ca
α	Steel, AISI 1045	8,000	3.9
β	Carbon Epoxy (61%)	1,900	1.1
γ	Steel, AISI 1045	8,000	3.9

Table 3 – Data for the cases involving real materials

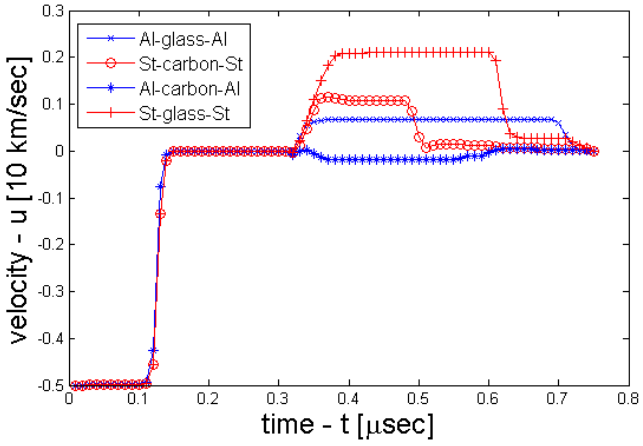

Figure 6 – Velocities over time at point A

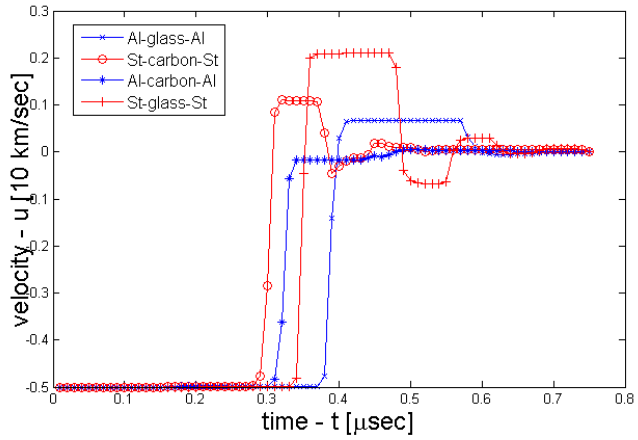

Figure 7 – Velocities over time at point B

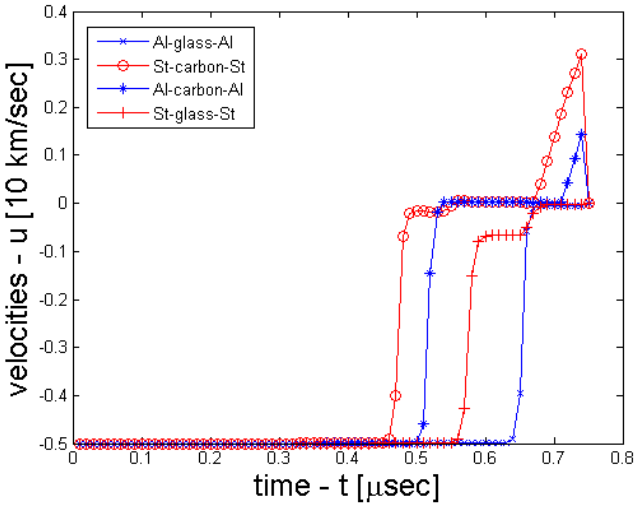

Figure 8 – Velocities over time at point C

The velocity induced shock propagates through the target material. At recoding point A (Fig.6), the effect of the transmission-reflection on the interface of the two materials is depicted. If a monolithic material was used, the velocity acquired by the material in the neighborhood of point A, after the shock wave passed, would not change. On the contrary, depending on the material, a shock wave can be delayed if the Ca number of the second material is high, as in the St-glass-St case, compared to the Al-carbon-Al case (Fig.6).

At point B (Fig.7), the rise-time for the shock in each material can be effectively considered to be the same, even though the maximum values span in a wide range, according to the material. The return of the velocity to negative values is attributed to the wave reflected on the β-α material surface.

At the last recording point C (Fig.8), towards the end of the process ($t > 0.65$) an expansion wave occurs due to the shock wave's reflection on the free boundary. This is not apparent for all materials.

Depending on the layered material's configuration, the reflection-transmission effects can be important. For the Al-carbon-Al case, each point's velocity is almost nullified by the shock wave, while the transmission-reflection effects for the St-glass-St case are severe (Fig.6 – Fig.8).

CONCLUSIONS

A modification of the standard SPH algorithm was suggested for layered materials under highly compressible effects. The overshoot at the impact point and unphysical blips appearing when shocks reach the interface of two materials were cured by the adding an artificial term in the continuity equation. It is considered to be a *holistic* approach, meaning that each particle interacts through the SPH kernel with the whole computational domain. Hence, no contact algorithm is needed for the interaction of different bodies or bodies including materials of different density under loading conditions mainly encountered during HVIs. Wave reflection-transmission patterns for layered materials can be recovered and studied.

The importance of taking into account the reflection-transmission phenomena for HVIs into layered materials was exhibited, along with the effects of different materials. From the four cases studied, only the Al-carbon-Al configuration could be described through a homogenized version of the structure; for the rest, the transmission-reflection effects seem to be too large to be neglected in a HVI simulation.

Further steps of development include the exploration of the proposed algorithm's properties and a method to obtain the α_ρ parameter's value. Benchmarking with the semi-analytical solution of the Riemann problem is also needed. Momentum conservation also must be investigated, although it was not found to be sensitive on the added dissipative term itself, rather on the varying smoothing length. Finally, extension to higher dimensions can be achieved after including the deviatoric part of the stress tensor.

Acknowledgments

This research was carried out under project number M11.4.10412 in the framework of the Research Program of the Materials innovation institute M2i (www.m2i.nl). It is also a research activity of Sioux LIME bv. (www.limebv.nl).

REFERENCES

[1] Drolshagen G., "Impact effects from small size meteoroids and space debris", Advances in Space Research **41**, pp.1123–1131, 2008.

[2] Whipple, F.L., "Meteorites and Space Travel", Astronomical Journal, **52**, 131, 1947.

[3] Christiansen, E.L., Crews, J.L., Williamsen, J.E., Robinson, J.H. and Nolen A.M., "Enhanced meteoroid and orbital debris shielding", International Journal of Impact Engineering, **17**, pp.217-228, 1995.

[4] Asay, J. R.and Kerley, G.I., "The response of materials to dynamic loading", International Journal of Impact Engineering,**5**, pp.69-99, 1984.

[5] Hiermaier, S.J.,*Structures Under Crash and Impact - Continuum Mechanics, Discretization and Experimental Characterization*, Chap. 3, pp.75, Springer Science+Business Media, LLC, New York, 2008.

[6] Davison, L., *Fundamentals of Shock Wave Propagation in Solids*, Chap. 8, pp.186-191, Springer-Verlag Berlin Heidelberg, 2008.

[7] Libersky, L.D., Petschek, A.G., Carney, T.C., Hipp, J.R. and Allandadi, F.A, "High strainLagrangian Hydrodynamics: A three-dimensional SPH code for dynamic material response", Journal of computational Physics, **109**, pp.67-75,1993.

[8] Hiermaier, S., Konke D., Stilp A.J. and Thoma K., "Computational simulation of the hypervelocity impact of Al-spheres on thin plates of different materials", International Journalof Impact Engineering, **20**, pp.363-374, 1997.

[9] Hayhurst, C.J., Livingstone, I.H., Clegg, R.A., Fairlie, G.E.,Hiermaier, S.J. and Lambert, M.,"Numerical Simulation of Hypervelocity Impacts on Aluminum and Nextel/Kevlar Whipple Shields", Hypervelocity Shielding Workshop, 8-11 March 1998, Galveston, Texas.

[10] Johnson, G.R., Stryk, R.A. and Beissel, S.R., "SPH for high velocity impact computations", Computer Methods in Applied Mechanics and Engineering, **139**, pp. 347-37, 1996.

[11] Campbell,J., Vignjevic, R. and Libersky L.,"A contact algorithm for smoothed particle hydrodynamics", Computer Methods in Applied Mechanicsand Engineering,**184**, pp. 49-65, 2000.

[12] Monaghan, J.J, and Ginold, R.A., Shock Simulation by the Particle Method SPH, journal of computational physics, **52**, pp. 374-389, 1983.

[13] Intuska S., "Reformulation of Smoothed Particle Hydrodynamicswith Riemann Solver", Journal of Computational Physics, **179**, pp.238-267, 2002.

[14] Cha, S.H. and Whitworth A.P., "Implementation and tests of Godunov-type particle hydrodynamics", Monthly Notices of the Royal Astronomical Society, **340**, pp. 73-90, 2003.

[15] Parshikov,A.N. and Medin S.A.,Smoothed Particle Hydrodynamics UsingInterparticle Contact Algorithms, Journal of Computational Physics,**180**, pp.358–382 2002.

[16] Riedel, W., Nahme, H., White, D. M., & Clegg, R. A., "Hypervelocity Impact Damage Prediction in Composites Part I & II", International Journal of Impact Engineering, **33**(1–12), pp.670–680, 2006.

[17] Clegg, R., Hayhurst,C., Leahy, J. and Deutekom, M.,"Application of a Coupled Anisotropic Material Model to High Velocity Impact Response of Composite Textile Armour", 18th International Symposium and Exhibition on Ballistics San Antonio, Texas USA, November 15-19 1999.

[18] Wicklein,M.,Ryana, S., Whiteb, D.M. andClegg, R.A., "Hypervelocity impact on CFRP: Testing, material modelling, and numerical simulation", International Journal of Impact Engineering,**35** (2008) pp.1861–1869.

[19] Hu, X.Y., Adams N.A.,"A multi-phase SPH method for macroscopic andmesoscopic flows", Journal of Computational Physics,**213**, (2006) pp. 844–861.

[20] Grenier, N., AntuonoM., Colagrossi,A., LeTouzé, D., and Alessandrini B.,"An Hamiltonian interface SPH formulation for multi-fluidand free surface flows", Journal of Computational Physics,**228,** pp.8380–8393, 2009.

[21] Colagrossi, A. and Landrini, M., "Numerical simulation of interfacial flows by smoothedparticle hydrodynamics", Journal of Computational Physics,**191**, pp.448–475, 2003.

[22] ZhangG.M. and Batra, R.C.,"Wave propagation in functionally graded materials by modified smoothed particle hydrodynamics (MSPH) method", Journal of Computational Physics,**222**, pp.374–390, 2007.

[23] Price, D.J., "Modelling discontinuities and Kelvin-Helmholtz instabilities in SPH", Journal of Computational Physics, **227**, pp.10040-10057, 2008.

[24] Monaghan, J.J, "SPH and Riemann Solvers", Journal of Computational physics,**136**, pp.298–307, 1997.

[25] Liu, M.B. and Liu, G.R., "Smoothed Particle Hydrodynamics (SPH): an Overview and Recent Developments", Archives of Computational Methods in Engineering, **17**, pp. 25–76, 2010.

PREVIOUS PUBLICATIONS IN THIS SERIES:

Number	Author(s)	Title	Month
13-05	J. de Graaf	Geodesics and connexions on matrix Lie groups	Febr. '13
13-06	S.P. Korzilius W.H.A. Schilders M.J.H. Anthonissen	An improved corrective smoothed particle method approximation for second-order derivatives	Apr. '13
13-07	M.E. Hochstenbach	Probabilistic upper bounds for the matrix two-norm	Apr. '13
13-08	M.E. Hochstenbach D.A. Singer P.F. Zachlin	Numerical approximation of the field of values of the inverse of a large matrix	Apr. '13
13-09	I. Zisis B.J. van der Linden C.G. Giannopapa	Towards a smoothed particle hydrodynamics algorithm for shocks through layered materials	May '13

Ontwerp: de Tantes,
Tobias Baanders, CWI